



Ionospheric local model and climatology from long-term databases of multiple incoherent scatter radars

Shun-Rong Zhang, John M. Holt, Anthony P. van Eyken, Mary Mccready,
Christine Amory-Mazaudier, Shoichiro Fukao, Michael Sulzer

► To cite this version:

Shun-Rong Zhang, John M. Holt, Anthony P. van Eyken, Mary Mccready, Christine Amory-Mazaudier, et al.. Ionospheric local model and climatology from long-term databases of multiple incoherent scatter radars. *Geophysical Research Letters*, 2005, 32 (20), pp.L20102. 10.1029/2005GL023603 . hal-00158334

HAL Id: hal-00158334

<https://hal.science/hal-00158334>

Submitted on 28 Jan 2016

HAL is a multi-disciplinary open access archive for the deposit and dissemination of scientific research documents, whether they are published or not. The documents may come from teaching and research institutions in France or abroad, or from public or private research centers.

L'archive ouverte pluridisciplinaire **HAL**, est destinée au dépôt et à la diffusion de documents scientifiques de niveau recherche, publiés ou non, émanant des établissements d'enseignement et de recherche français ou étrangers, des laboratoires publics ou privés.

Ionospheric local model and climatology from long-term databases of multiple incoherent scatter radars

Shun-Rong Zhang,¹ John M. Holt,¹ Anthony P. van Eyken,² Mary McCready,³ Christine Amory-Mazaudier,⁴ Shoichiro Fukao,⁵ and Michael Sulzer⁶

Received 23 May 2005; revised 10 August 2005; accepted 20 September 2005; published 25 October 2005.

[1] Empirical ionospheric local models have been developed from long-term data sets of seven incoherent scatter radars spanning invariant latitudes from 25° to 75° in American, European and Asian longitudes at Svalbard, Tromsø, Sondrestrom, Millstone Hill, St. Santin, Arecibo and Shigaraki. These models, as important complements to global models, represent electron density, ion and electron temperatures, and ion drifts in the E and F regions, giving a comprehensive quantitative description of ionospheric properties. A case study of annual ionospheric variations in electron density and ion temperature is presented based on some of these models. Clear latitudinal, longitudinal, and altitude dependency of annual and semiannual components are found. **Citation:** Zhang, S.-R., J. M. Holt, A. P. van Eyken, M. McCready, C. Amory-Mazaudier, S. Fukao, and M. Sulzer (2005), Ionospheric local model and climatology from long-term databases of multiple incoherent scatter radars, *Geophys. Res. Lett.*, 32, L20102, doi:10.1029/2005GL023603.

1. Introduction

[2] Long-term incoherent scatter radar (ISR) observations provide an extremely valuable data source for addressing significant scientific issues related to ionospheric and thermospheric climatology. The altitude dependence, for instance, of various variations in the electron density, thermal status, and dynamics are subjects not well suited for other instruments on the ground or on satellites to pursue in a comprehensive manner. Since the development of incoherent scatter radars in the 1960's, a long-term observational data set has been accumulating. Among the existing nine operational ISRs, over 30 years worth of data in modern digital form are available from Arecibo and Millstone Hill radars and over 7 years worth of data are available for the Svalbard radar; other sites, including the St. Santin radar, which was closed in 1986, encompass at least one solar cycle. Table 1 lists the ISR sites and the time coverage of the data included in this study.

[3] Empirical models are important tools for many research efforts. The International Reference Ionosphere (IRI) [Bilitza, 2001], as a global ionospheric model, has been used widely. Its electron density component was derived largely from ionosonde observations, in particular, the peak density and its height as well as the height variation at the bottomside, whereas very few ISR profiles have been taken into account. ISR provides important information about the E-valley structure, which can not be accurately deduced from ionosondes. The IRI's plasma temperature component was contributed by satellite data (of course with limited height variations) and by some ISR data which, however, came from earlier observations from the 1970–80's. Local empirical models from long-term data sets have many important aspects, such as validating theoretical and empirical global models (see *Zhang and Holt* [2004] and *Zhang et al.* [2004] for some initial comparisons between the ISR and IRI models); as average models they can be also used for ionospheric climatology studies, as we shall present here. *Holt et al.* [2002] have recently reported local and regional models based on Millstone Hill ISR data. *Zhang and Holt* [2004] and *Zhang et al.* [2004] have reported plasma temperature climatology and model studies for Millstone Hill and St. Santin. The present work represents a substantial development in modeling Ne, Ti, Te and ion drifts from ISR observations at seven sites spanning invariant latitudes from 25° to 75°. Presented as examples of model outputs are results for the annual and semiannual ionospheric variations of the modeled parameters.

[4] The annual variation of ionospheric electron density Ne is largely caused by the annual change of solar zenith angle and of the neutral composition. Prior studies based on ionosonde and TEC data and theoretical modeling have indicated the variation of annual changes with longitude and latitude [Fuller-Rowell et al., 1996; Millward et al., 1996; Rishbeth, 1998, and references therein]. ISR data at Shigaraki showed the variation with height in the F region [Balan et al., 1998; Kawamura et al., 2002]. Further studies are needed to resolve issues on the altitude dependence for multiple parameters. A long-term database from a variety of latitudes and longitudes covering an appropriate altitude range is essential, and has been considered in this paper.

2. Data and Modeling

[5] We use data from the Madrigal distributed data system. Table 1 lists the time coverage of data for each site. As this study is concerned primarily about local measurements for the E and F regions, we select data between 100–650 km height for most sites (up to 1000 km for Millstone) from radars' high elevation (EL)

¹Haystack Observatory, Massachusetts Institute of Technology, Westford, Massachusetts, USA.

²EISCAT Scientific Association, Kiruna, Sweden.

³SRI International, Menlo Park, California, USA.

⁴Centre for the Study of Earth and Planets Environments, Centre National de la Recherche Scientifique, Saint-Maur-des-Fossés, France.

⁵Research Institute for Sustainable Humanosphere, Kyoto University, Uji, Japan.

⁶Arecibo Observatory, National Astronomy and Ionosphere Center, Puerto Rico.

Table 1. Incoherent Scatter Radars and Data^a

Station	Lat., deg	Lon., deg	Inv., deg	Coverage
Svalbard	78.1	16.0	74.9	1997–
Sondrestrom	67.0	309.0	73.2	1990–
Tromsø	69.6	19.2	66.4	1984–
Millstone	42.6	288.5	53.4	1970–
St. Santin	44.6	2.2	46.3	1973–85
Arecibo	18.3	293.2	32.2	1966–
Shigaraki	34.8	136.1	24.5	1986–

^aLat. and Lon. are geodetic latitude and longitude. Inv. is invariant latitude.

measurements. Data from Svalbard Radar (operational since 1996) and Tromsø UHF and VHF (1981) Radars are from EISCAT Common Program (CP) experiments with $EL \geq 75^\circ$. Sondrestrom radar (1983) data are from its ACPORT files corresponding to a variety of antenna modes with $EL \geq 80^\circ$, and its 16-baud alternating code data are all excluded. Millstone Hill radar (1960) data contain all experiments from both zenith and steerable antennas with $EL \geq 45^\circ$. St. Santin data are from both bistatic and quadristatic measurements from Nancay as well as the Montpazier and Mende receivers. Arecibo Radar (1963) data are largely from its World Day experiments. Shigaraki Middle and Upper Atmosphere (MU) Radar (1986) data contain all experiments obtained with its power profile, 4-pulse temperature and 2-pulse line-of-sight modes; due to frequent contamination of meteoric echoes, we exclude data <200 km height, therefore producing only the F2 region models. Using a variety of pulse lengths, these radars provide typically 25–50 km height resolution for the F region observations, and 10–15 km height resolution for the E region observations. Most temperature and velocity data and some electron density data come with an error estimate; for those without the error we assign a large value close to the maximum error in the corresponding data. The modeling procedure takes into account these errors.

[6] Model parameters are Ne, Te and Ti. Parallel ion drift models are also developed for Sondrestrom, Millstone and Arecibo. The modeling technique is an improved version of Holt *et al.* [2002] and is similar to that of Zhang *et al.* [2004]. The data for each site are binned by month and local time with 3-month and 1-hour bin sizes. Assuming a linear variation between any two consecutive altitude nodes (piecewise-linear function), we obtain linear coefficients for the height variation. These coefficients are assumed to be linear in the solar activity index F10.7 and magnetic activity index 3-hourly ap, where F10.7 is for the previous day and ap is for the previous 3 hours [Hedin, 1983; Hecht *et al.*, 1991]. The choice of the previous day's F10.7 was based on work by Buonsanto and Pohlman [1998] and Roemer [1967] who suggested that the thermospheric response time to the solar activity is nearly 1 day. Tests with Millstone Ne, Te and Ti data spanning about 3 solar cycles show that the correlations of each parameter with different F10.7 values (for the current day, 1 or more days earlier, and 81-day averages) are not significantly different. Therefore we use the previous day's F10.7 in accord with prior studies. The use of ap index here represents a simple approach to representing the magnetic activity controls on the ionosphere. A more sophisticated approach, however, is

to consider the time history of magnetic activity effects, such as that developed by Araujo-Pradere *et al.* [2002] for the F2 peak density modeling during storms. Similar consideration should be taken into account in our future update when sufficient storm time ISR data have been collected.

[7] The height nodes are at 100, 110, 120, 130, 140, 160, 180, 200, 225, 250, 300, 350, 400, 450, 500, 550, and 600 km, except for Millstone with additional 700 and 1000 km nodes, and for Shigaraki with nodes between 200–600 km at a very fine 10/20 km spacing below/above 400 km because of the use of the Barker-coded power profile experiments. These nodes apply to all parameters, except for Shigaraki where Te and Ti profiles have nine nodes at 230, 275, 320, 365, 410, 455, 500, 545, 590 km, corresponding to average altitudes of gates used in the standard MU radar 4-pulse measurement. Due to the relatively limited amount of plasma temperature data for MU radar, we have used a 3-hour bin size to improve the statistics.

[8] A sequential least squares fit to the solar activity dependence and piecewise-linear altitude dependence functions is performed, generating coefficients for the constant, F10.7 and ap terms for each of the 12 (monthly bins) \times 24 (hourly bins) = 288 bins and each of altitude nodes. To further smooth diurnal and seasonal variations, we apply a 3 (month) \times 3 (hour) median filter in season and local time to the coefficients. Lastly, a cubic B-spline is fit to give twice-differentiable height variations, a feature very useful for height gradient calculations.

3. Annual Variations

[9] As an example of the model output, annual electron density variations vs height, as shown in Figure 1, are calculated for noon with F10.7 = 135 and ap = 15 representing conditions of median solar activity during quiet magnetic activity. The upper atmosphere meridional circulations, caused by upwelling due to solar EUV heating and auroral heating, result in latitudinal and annual/semiannual changes of the composition [Rishbeth, 1998]. In the auroral and polar cap area (Svalbard), while auroral heating appears persistently over the year and the O/N₂ ratio shows less winter-summer difference, the annual variation of the solar zenith angle plays a major role so that there is a simple annual change with maximum Ne in summer. Tromsø, at a lower latitude, shows lower Ne in summer than in winter (“winter anomaly”) with the highest in equinox (semiannual changes). The winter anomaly in Ne is an indication of the large winter-summer composition difference with O/N₂ higher in winter. St. Santin, at midlatitudes in the same longitude sector, shows well defined semiannual changes with Ne higher in early March than in late October (equinoctial asymmetry), in addition to the winter anomaly. The asymmetry is particularly pronounced above the F2 peak heights.

[10] In the American sector, Sondrestrom has just a slightly lower invariant latitude and a much lower geodetic latitude than Svalbard, however, a well defined semiannual variation is seen with a similar equinoctial asymmetry but higher F2 peak heights as compared to Tromsø at nearly an identical geodetic latitude. Such a semiannual variation may be caused by the combined effect of annual changes in the

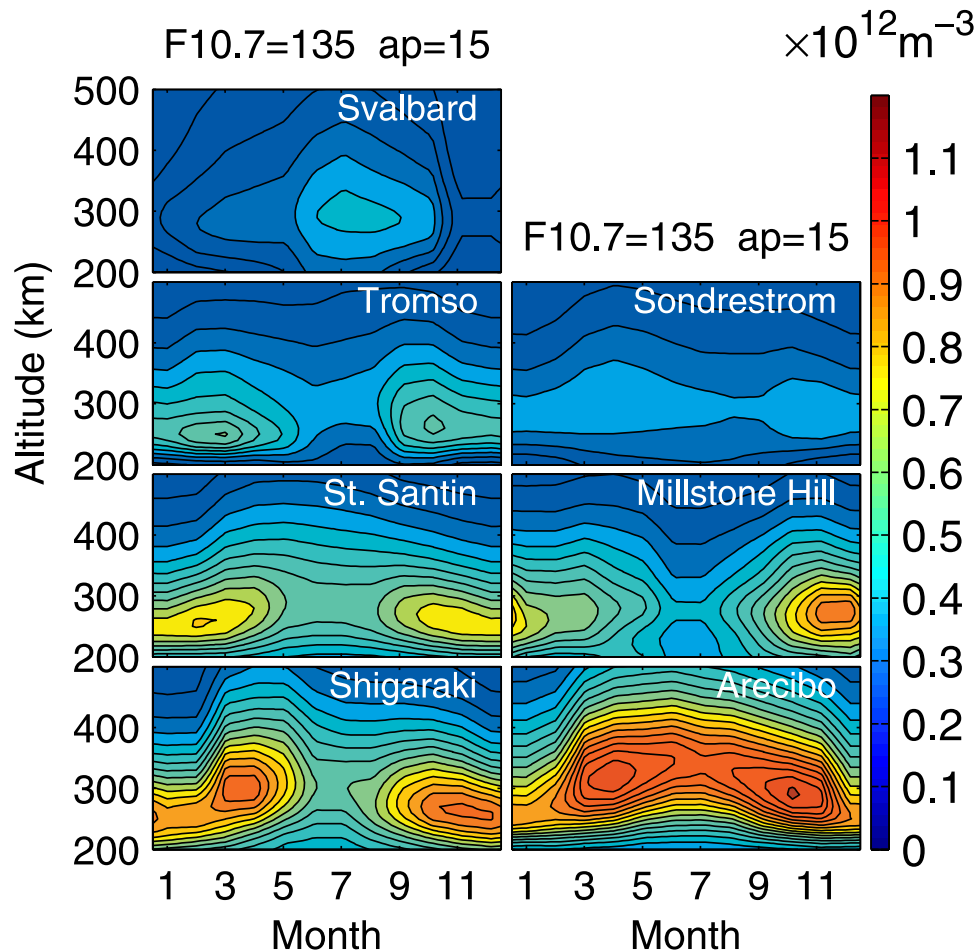


Figure 1. Model representations of annual electron density variations vs height in the F region. Contours are given at $6 \times 10^{10} \text{ m}^{-3}$ interval for up to $1.2 \times 10^{12} \text{ m}^{-3}$. The month tick indicates approximately where the central day of the month is.

solar zenith angle and in the composition, which may be in the middle way between Svalbard and Tromsø. Millstone Hill, with a similar geodetic latitude but in the subauroral area as compared to St. Santin, tends to show a prominent winter anomaly as well as higher Ne in the second half of the year. The semiannual component is larger above the peak height. Ne is lower in American longitudes (Sondrestrom and Millstone; excluding in winter for Millstone) than in European ones (Tromsø and St. Santin). This might be due to their higher magnetic latitudes causing lower O/N_2 . Well defined semiannual patterns occur at Arecibo and Shigaraki at lower midlatitudes. Magnetic latitudes for both sites are $\sim 28^\circ$, however, Arecibo receives stronger solar irradiation as it is in the equatorial side of the tropic zone; therefore Ne is higher. The equinoctial asymmetry is most evident at Shigaraki [Balan *et al.*, 1998]. Ne above the F2 peak appears higher in spring than in autumn over those mid- and lower mid-latitudes, with a noticeable exception at Millstone Hill.

[11] Neutral winds also modify the semiannual variation directly through moving ions to regions of higher or lower loss rates thus decreasing or increasing Ne [Balan *et al.*, 1998; Kawamura *et al.*, 2002], and indirectly through atmospheric prevailing flows carrying the neutral gas of rich nitrogen [Rishbeth, 1998]. Effects of winds

and composition should vary with altitude regimes. The somewhat unusual behavior of higher Ne in the second half of the year at Millstone needs further investigations, which may require neutral composition and wind information specific for the region. Such information on the neutral atmosphere may be partly obtainable from the ISR long-term database. However, the height of the F2 peak, suggestive of the meridional neutral wind, differs little over the year indicating no or only weak equinoctial asymmetry in the wind.

[12] On the other hand, variations in Ti and the neutral temperature can provide some hints about the composition if the upper atmosphere is assumed to be in diffusive equilibrium as expressed in the Bates function. A higher neutral temperature implies a larger scale height and lower O/N_2 . Figure 2 shows annual Ti variations for three sites. (Results for Shigaraki showed a semiannual component in Ti [see Balan *et al.*, 1998].) At Svalbard and Tromsø, Ti is highest in summer. At Millstone the maximum occurs in later spring and earlier summer (May). Ti at around 250–300 km is a good measure of the exospheric temperature for midlatitudes [Buonsanto and Pohlman, 1998], thus we might expect the atmospheric asymmetry about summer with a corresponding maximum neutral temperature and lowest O/N_2 in May,

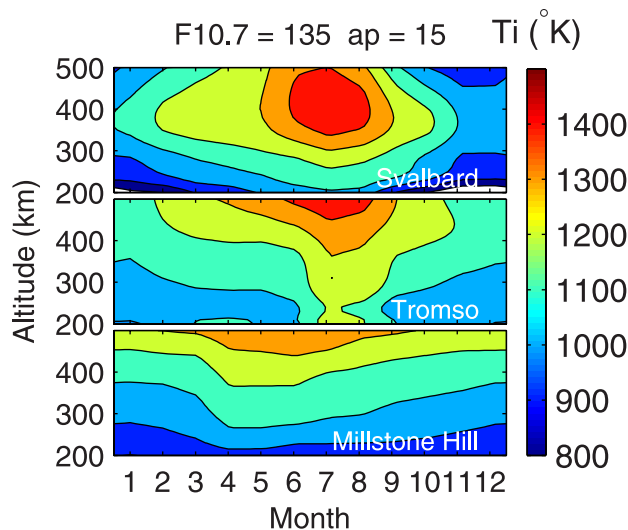


Figure 2. Model representations of annual ion temperature variations vs height in the F region.

contributing to the equinoctial asymmetry in Ne mentioned above.

4. Summary

[13] Local empirical ionospheric models have been developed from long-term data sets of seven ISRs in American, European and Asian longitudes at Svalbard, Tromsø, Sondrestrom, Millstone Hill, St. Santin, Arecibo and Shigaraki. These models, as important complements to global models such as IRI, represent Ne, Te, Ti and ion drifts in the E and F regions, giving a quantitative description of ionospheric properties. A case study of annual variations is presented based on some of these models. Clear latitudinal, longitudinal, and altitude dependency of annual and semi-annual components are found. The models are available from the authors or on-line at <http://www.openmadrigal.org>, where virtual ISRs for each site are also provided based on these models and near real-time values of F10.7 and ap.

[14] **Acknowledgments.** We thank the staff at EISCAT, Svalbard, Sondrestrom, and in particular, Bill Wrideout and members of the Haystack Observatory Atmospheric Sciences Group for assembling and maintaining the Madrigal database. We thank S. Kawamura for preparing the MU radar data. A. Zalucha and A. Brooks have been involved in model developments for St. Santin and Arecibo as REU students. This research was supported by NSF Space Weather grant ATM-0207748. The Sondrestrom, Millstone Hill, and Arecibo incoherent scatter radars are supported by the U.S. National Science Foundation. EISCAT is an international association supported by the research councils of Finland (SA), France (CARS), Germany (MPG), Japan (NIPR), Norway (NFR), Sweden (VR), and the United Kingdom (PPARC). The MU radar belongs to and is operated by the Research

Institute for Sustainable Humanosphere of Kyoto University. St. Santin and Arecibo data are imported from the CEDAR database.

References

- Araujo-Pradere, E. A., T. J. Fuller-Rowell, and M. V. Codrescu (2002), STORM: An empirical storm-time ionospheric correction model: 1. Model description, *Radio Sci.*, **37**(5), 1070, doi:10.1029/2001RS002467.
- Balan, N., Y. Otsuka, S. Fukao, and G. J. Bailey (1998), Equinoctial asymmetries in the ionosphere and thermosphere observed by the MU radar, *J. Geophys. Res.*, **103**, 9481–9486.
- Bilitza, D. (2001), International Reference Ionosphere 2000, *Radio Sci.*, **36**, 261–275.
- Buonsanto, M. J., and L. M. Pohlman (1998), Climatology of neutral exospheric temperature above Millstone Hill, *J. Geophys. Res.*, **103**, 23,381–23,392.
- Fuller-Rowell, T. J., M. V. Codrescu, H. Rishbeth, R. J. Moffett, and S. Quegan (1996), On the seasonal response of the thermosphere and ionosphere to geomagnetic storms, *J. Geophys. Res.*, **101**, 2343–2353.
- Hecht, J. H., D. J. Strickland, A. B. Christensen, D. C. Kayser, and R. L. Walterscheid (1991), Lower thermospheric composition changes derived from optical and radar data taken at Sondre Stromfjord during the great magnetic storm of February, 1986, *J. Geophys. Res.*, **96**, 5757–5776.
- Hedin, A. E. (1983), A revised thermospheric model based on mass spectrometer and incoherent scatter data: MSIS-83, *J. Geophys. Res.*, **88**, 10,170–10,188.
- Holt, J. M., S.-R. Zhang, and M. J. Buonsanto (2002), Regional and local ionospheric models based on Millstone Hill incoherent scatter radar data, *Geophys. Res. Lett.*, **29**(8), 1207, doi:10.1029/2002GL014678.
- Kawamura, S., N. Balan, Y. Otsuka, and S. Fukao (2002), Annual and semiannual variations of the midlatitude ionosphere under low solar activity, *J. Geophys. Res.*, **107**(A8), 1166, doi:10.1029/2001JA000267.
- Millward, G. H., H. Rishbeth, T. J. Fuller-Rowell, A. D. Aylward, S. Quegan, and R. J. Moffett (1996), Ionospheric F2 layer seasonal and semiannual variations, *J. Geophys. Res.*, **101**, 5149–5156.
- Rishbeth, H. (1998), How the thermospheric circulation affects the ionospheric F2-layer, *J. Atmos. Sol. Terr. Phys.*, **60**, 1385–1402.
- Roemer, M. (1967), Geomagnetic activity effect and 27-day variation: Response time of the thermosphere and lower exosphere, *Space Res.*, **7**, 1091–1099.
- Zhang, S.-R., and J. M. Holt (2004), Ionospheric temperature variations during 1976–2001 over Millstone Hill, *Adv. Space Res.*, **33**, 963–969, doi:10.1016/j.asr.2003.07.012.
- Zhang, S.-R., J. M. Holt, A. M. Zalucha, and C. Amory-Mazaudier (2004), Mid-latitude ionospheric plasma temperature climatology and empirical model based on Saint Santin incoherent scatter radar data from 1966–1987, *J. Geophys. Res.*, **109**, A11311, doi:10.1029/2004JA010709.
- C. Amory-Mazaudier, Centre for the Study of Earth and Planets Environments, CNRS, F-94107 Saint-Maur-des-Fossés Cedex, France. (christine.mazaudier@cetp.ipsl.fr)
- S. Fukao, Research Institute for Sustainable Humanosphere, Kyoto University, Uji, Kyoto 611-0011, Japan. (fukao@rish.kyoto-u.ac.jp)
- J. M. Holt and S.-R. Zhang, Haystack Observatory, Massachusetts Institute of Technology, Route 40, Westford, MA 01886, USA. (jmh@haystack.mit.edu; shunrong@haystack.mit.edu)
- M. McCready, SRI International, Menlo Park, CA 94025, USA. (marry.mccready@sri.com)
- M. Sulzer, Arecibo Observatory, National Astronomy and Ionosphere Center, HC03 Box 53995, Arecibo, PR 00612. (sulzer@naic.edu)
- A. P. van Eyken, EISCAT Scientific Association, P.O. Box 164, SE-981 23, Kiruna, Sweden. (tony.van.eyken@eiscat.com)